



**POLITECNICO**  
MILANO 1863

SCUOLA DI INGEGNERIA INDUSTRIALE  
E DELL'INFORMAZIONE

EXECUTIVE SUMMARY OF THE THESIS

## Pressure and strain effects on cuprate superconductors from first principles calculations

LAUREA MAGISTRALE IN ENGINEERING PHYSICS- INGEGNERIA FISICA

**Author:** PIETRO NICOLÒ BRANGI

**Advisor:** PROF. GIACOMO CLAUDIO GHIRINGHELLI

**Co-advisor:** PROF. GIANNI PROFETA

**Academic year:** 2022-2023

---

### 1. Introduction

High temperature superconductivity in cuprate perovskites was discovered in 1986 and has represented an outstanding challenge for physicists ever since. Understanding the physical origin of superconductivity up to temperatures of 135 K has been a primary objective for both experimentalists and theorists all over the world but, despite all of the noticeable progress that has been made, a clear and complete description of cuprates' physics is still lacking.

This work tries to move a step forward in the theoretical *ab initio* description of cuprate superconductors, which has been one of the main struggles in this field. The development of a theory capable of predicting in a quantitative way the physical properties of these compounds would be a great advancement not only from the basic physics point of view but also technologically: it could allow to do material screening and predict new compounds with higher critical temperatures  $T_c$  or to tailor the characteristics of existing materials in order to achieve the desired properties.

The formalism used to compute the properties of the materials object of this work is the Density Functional Theory (DFT). DFT is an incredibly

powerful instrument for solid state physics that allows to make precise calculations on real materials. However, this theoretical tool wasn't able to predict the properties of any cuprate material, not even in its normal state, up until very recent times, when new exchange-correlation functionals were developed. The recently introduced SCAN (Strongly Constrained and Appropriately Normed) functional has represented a remarkable improvement for the calculations on cuprates over other very popular ones. Indeed, soon after its development, it was made clear by some works [1] that the SCAN was capable of predicting a good portion of the normal state phenomenology of cuprate materials, such as the antiferromagnetic and insulating behaviour of the undoped model cuprate  $\text{La}_2\text{CuO}_4$  (LCO) and its insulator-metal phase transition when doped with Sr in the compound  $\text{La}_{2-x}\text{Sr}_x\text{CuO}_4$  (LSCO). These results have been encouraging for studying other properties of cuprates materials using this new theoretical instrument. That is what is done in this work, first by reproducing the established results reported in the reference paper [1], then by calculating the structural, electronic and magnetic properties of LCO under hydrostatic pressure and biaxial strain. The

obtained results are then compared to recent experimental results to confirm the outcome of the calculations.

## 2. DFT exchange-correlation functionals

The theoretical-computational instrument used throughout this work is the density functional theory in the Kohn-Sham (KS) approach, as implemented in the Vienna Ab-initio Simulation Package (VASP). DFT is an incredibly powerful instrument for the calculation of the properties of solid state matter, based on the two Hohenberg and Kohn theorems, according to which all the ground state properties of a system of electrons in an external potential (such as the one of the nuclei) are determined by the electron density function  $n(\mathbf{r})$ . Within the Kohn-Sham approach, then, the interacting electrons system is mapped on a fictitious independent electron system where all the complexity given by electronic correlations is contained in the exchange-correlation energy term, the expression of which is generally not known.

The strong electronic correlations in cuprate materials are what made it hard to reproduce their behaviour with local energy functionals.

### 2.1. SCAN functional

The SCAN functional belongs to the family of the so-called "meta-GGA" functionals. These take one step further in the expression of the exchange-correlation energy density  $\epsilon_{xc}$ . The exchange-correlation energy  $E_{xc}$  can be indeed formally written as

$$E_{xc}[n_{\uparrow}, n_{\downarrow}] = \int d\mathbf{r} n(\mathbf{r}) \epsilon_{xc}(n_{\uparrow}, n_{\downarrow}, \nabla n_{\uparrow}, \nabla n_{\downarrow}, \tau_{\uparrow}, \tau_{\downarrow})$$

where  $n_{\uparrow}(\mathbf{r})$  and  $n_{\downarrow}(\mathbf{r})$  are respectively the up and down electron spin densities and the total electron density is the sum of the two:  $n(\mathbf{r}) = n_{\downarrow}(\mathbf{r}) + n_{\uparrow}(\mathbf{r})$ .

In the case of the free electron gas mentioned above, within the Local Spin Density Approximation (LSDA),  $\epsilon_{xc}$  only depends on  $n_{\uparrow}(\mathbf{r})$  and  $n_{\downarrow}(\mathbf{r})$ , whereas in the Generalized Gradient Approximation (GGA) the dependence of  $\epsilon_{xc}$  on the gradient of the two electron spin densities is added in. Meta-GGA functionals also include a dependence on the laplacian on the electron density,  $\nabla^2 n$ , which in this case appears in

the form of the orbital kinetic energy density  $\tau_{\sigma} = \sum_i^{occ} (1/2) |\nabla \psi_{i,\sigma}|^2$ . This addition allows the meta-GGA functionals to satisfy all of the known constraints on the exchange-correlation functional: that is the main difference of the SCAN with respect to all the previously developed functionals, it manages to satisfy all 17 known exact constraints that a meta-GGA can satisfy [2].

## 3. Unstrained LCO properties

The results reported in Ref. [1] were a very encouraging first step towards an *ab initio* treatment of cuprate materials, demonstrating that the SCAN functional correctly predicts with very good accuracy the structural and electronic properties of LSCO and of its parent compound. LCO has a tetragonal or orthorhombic crystal structure depending on the temperature and it is characterized by the presence of copper oxide  $\text{CuO}_2$  planes as all cuprates, alternating with insulating *La* interlayers. One of the main features of the crystal structure is the coordination of the copper atoms with the oxygens, with the formation of  $\text{CuO}_6$  octahedra as one can see in Figure 1.

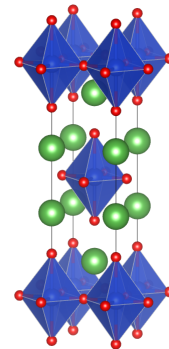
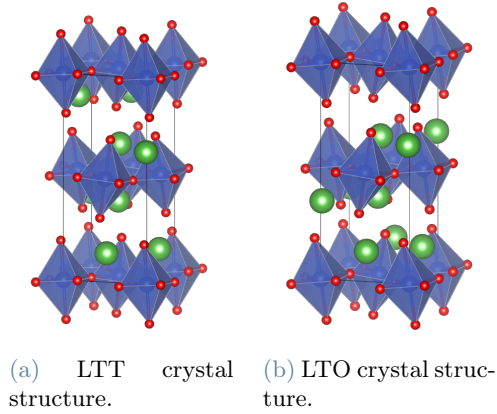


Figure 1: Unit cell of LCO in the HTT crystal phase. One can easily see the blue  $\text{CuO}_6$  octahedra.

The parent compound is experimentally found to exhibit three different crystal phases that differ by unit cell symmetry and octahedral tilting: the High Temperature Tetragonal (HTT) crystal phase has the octahedra axially aligned and the unit cell has a tetragonal symmetry (see Figure 1), the Low Temperature Tetragonal (LTT) still retains the tetragonal symmetry but the octahedra are tilted along

the (110) direction in alternate ways in the  $\text{CuO}_2$  plane (see Figure 2a) and finally the Low Temperature Orthorhombic has the octahedra tilted along the (100) direction (see Figure 2b).



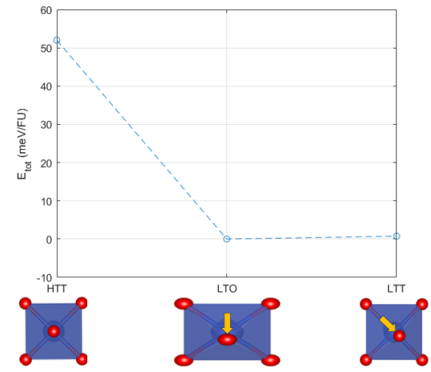
**Figure 2:** LTT and LTO crystal structure. One can see that to allow for the octahedral tilting, alternated in opposite ways in the  $\text{CuO}_2$  planes, the unit cell is enlarged to a  $\sqrt{2} \times \sqrt{2}R45^\circ$  one.

The LTO and LTT crystal phases also exhibit an in-plane antiferromagnetic ordering with the central coppers of the octahedra tilted in different ways having opposite magnetic moment.

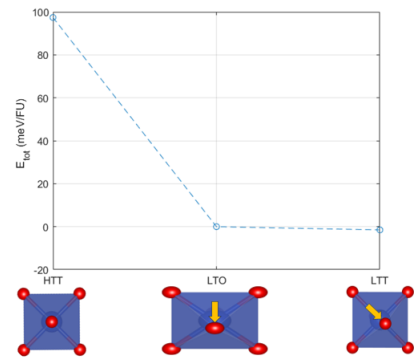
We calculated the structural electronic and magnetic ground state properties of LCO using both PBE and SCAN functionals, finding that the LTO crystal structure is the ground state of the system at low temperatures, according to the results with the SCAN functional, with the LTT just above that, whereas the HTT is the highest energy one (see Figure 3a). The PBE functional yields a similar result, but with the LTT phase at slightly lower energy than the LTO (see Figure 3b).

The lattice constants are also predicted accurately by the SCAN, as well as the magnetic moments on the  $\text{Cu}$  atoms, as one can see in Figure 4.

We then calculated the band structure for the three phases of LCO and the corresponding Densities Of States (DOS), which confirm that the SCAN functional correctly predicts LCO to be an insulator with the conduction and valence bands having primarily a  $\text{Cu-}d_{x^2-y^2}$  and  $\text{O-}p_x-p_y$  character, as expected from a simple tight bind-



(a) SCAN phase comparison.



(b) PBE phase comparison.

**Figure 3:** Energy comparison of the three phases. The cartoons of the octahedra highlight the tilt mode and the orthorhombic symmetry (of the unit cell) in the LTO phase.

ing picture (see Figure 5).

In the doped compounds the antiferromagnetic order is destroyed and the material becomes metallic, with one band crossing the Fermi level providing the electrons for Cooper pairing. We thus report in Figure 6 the band structure of non-magnetic LCO in the tetragonal phase using the SCAN functional. The SCAN band is comparable with the one obtained with the PBE functional with the exception of the distance of the valence band from the Fermi level at the X point. This result can be important since this band represents the starting point for model calculations on the superconducting phase.

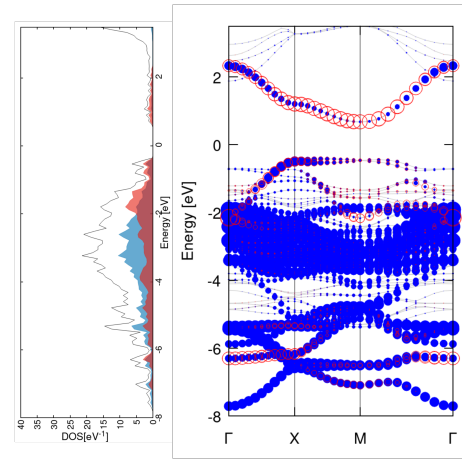
#### 4. LCO properties under biaxial strain

The effect of strain on the superconducting properties of cuprate thin films is well known since

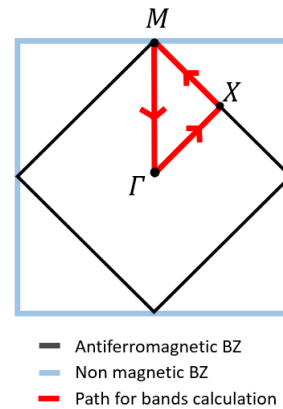
		SCAN				Experiment		
		LTO	LTT	HTT	HTT (NM)	LTO	LTT	HTT
Cell volume	$V[\text{\AA}^3]$	380	380	376	188	379.1	380.3	384.2
Lattice parameters	$a[\text{\AA}]$	5.329	5.390	5.351	3.782	5.335	5.360	5.391
	$b[\text{\AA}]$	5.461	-	-	-	5.421	5.360	5.391
	$c[\text{\AA}]$	13.057	13.079	13.131	13.145	13.107	13.236	13.219
Cu magnetic moment	$[\mu_B]$	0.510	0.511	0.500	0	0.495	-	-

Figure 4: Lattice parameters predicted with the SCAN functional by our calculations compared to the experimentally measured ones.

the publication of a seminal article by Locquet and others [3] where a doubled  $T_c$  in compressively strained  $\text{La}_{1.9}\text{Sr}_{0.1}\text{CuO}_4$  is reported. This impressive result paved the way for further studies on the topic, given that the microscopic origin of such a marked increase was still unclear. We studied the electronic and magnetic properties of LCO under biaxial strain, in an attempt to predict the experimental results reported in a more recent paper by Ivashko and others [4], where the microscopic origin for the increase in  $T_c$  is identified in the increased exchange coupling  $J$  between copper atoms. In that work  $J$  is studied as a function of the strain applied to a thin film of LCO, grown on different substrates, reporting a linear decrease of  $J$  with the strain  $\epsilon$  (notice that  $\epsilon < 0$  is compressive strain). By calculating the energies of the strained system (in the LTT crystal phase) in the antiferromagnetic and ferromagnetic phases we compute  $J$ , according to the Heisenberg Hamiltonian, as the difference between the two energies. Indeed considering first neighbours we have that the magnetic energy per unit cell per  $\text{CuO}_2$  plane is:  $E = \sum_{\langle i,j \rangle} J \mathbf{S}_i \cdot \mathbf{S}_j = 4JS^2$ . Then by considering the presence of two planes per unit cell the difference in energy between the ferromagnetic and antiferromagnetic states results proportional to  $J$ :  $\Delta E_{tot}^{FM-AFM} = 8JS^2 - (-8JS^2) = 16JS^2$ , with  $S = 1/2$ . The results of the calculations are qualitatively similar to those reported in Ref. [4] with a linear decrease of  $J$  with  $\epsilon$ . Our results are in line with those in the literature that measure  $J$  at zero strain [5].



(a) DOS and band structure of the LTT phase of LCO. The blue filled circles represent the strength of the projection of the state on the  $O-p_x-p_y$  orbitals, the red unfilled circles represent the strength of the projection of the state on the  $\text{Cu}-d_{x^2-y^2}$  orbitals. The same color coding is applied for the DOS.



(b) Brillouin zone of the magnetic and non magnetic unit cells. In red the path followed for the calculation of the energy bands.

Figure 5

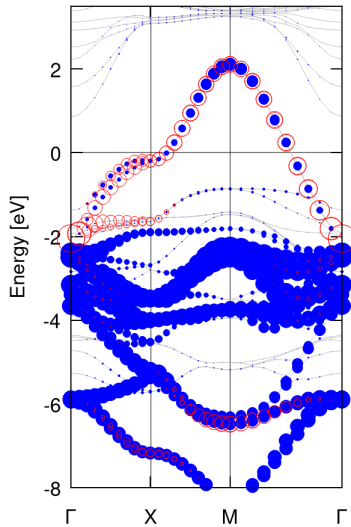


Figure 6: Band structure of the non magnetic phase calculated with the SCAN functional.

We have found that at higher strain values the ferromagnetic state becomes unstable, thus the method employed for the calculation of  $J$  is formally no longer applicable.

We also calculated the band structure of the antiferromagnetic phase as a function of the strain obtaining an interesting change in the band character at the  $X$  point that could be further investigated.

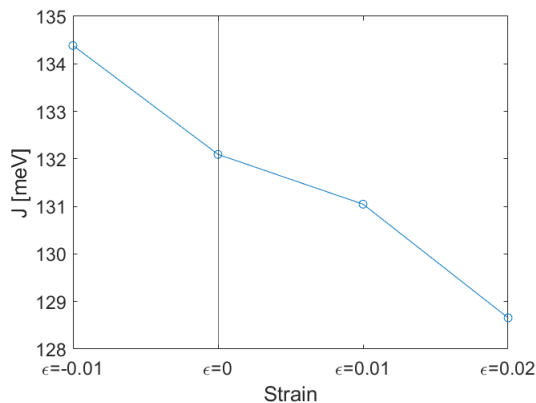


Figure 7: Exchange coupling  $J$  as a function of the strain  $\epsilon$  from DFT calculations with the SCAN functional.

## 5. LCO properties under hydrostatic pressure

We then turned our attention to the properties of LCO under hydrostatic pressure. In a

recent work Calamitou and others [6] studied the structural properties of LCO under pressure, highlighting a structural phase transition from the orthorhombic to the tetragonal phase taking place at around 10 GPa. The most evident feature of this phase transition is the discontinuity in the derivative of the  $c/a$  ratio between the lattice constant in the  $z$  direction and the in-plane one (see Figure 8b). We computed the ratio for LCO at various unit cell volumes (and correspondingly pressures) finding a remarkable agreement with the experiments. The calculations highlight the phase transition at around 13 GPa (see Figure 8). We also computed the P-V equation of state of LCO by fitting the computed  $E(V)$  function with the Birch-Murnaghan equation of state:  $E(V) = E_0 + \frac{9V_0 B_0}{16} \left\{ \left[ \left( \frac{V_0}{V} \right)^{2/3} - 1 \right]^3 B'_0 + \left[ \left( \frac{V_0}{V} \right)^{2/3} - 1 \right]^2 [6 - 4 \left( \frac{V_0}{V} \right)^{2/3}] \right\}$  obtaining the bulk modulus and its derivative which can be used in the P-V Birch-Murnaghan equation of state:  $P(V) = \frac{3B_0}{2} \left[ \left( \frac{V_0}{V} \right)^{7/3} - \left( \frac{V_0}{V} \right)^{5/3} \right] \left\{ 1 + \frac{3}{4} (B'_0 - 4) \left[ \left( \frac{V_0}{V} \right)^{2/3} - 1 \right] \right\}$ . By comparing the calculations to the experimental data we find an almost perfect agreement of the *ab initio* calculation with the experimental data (see Figure 9).

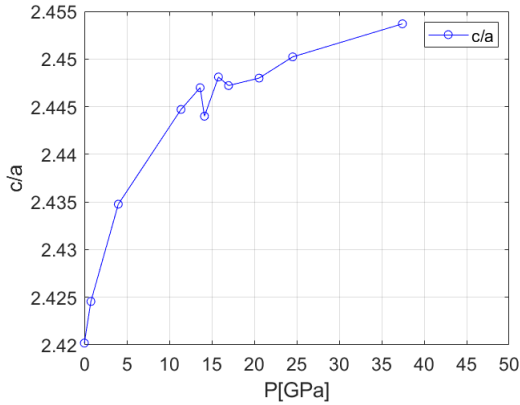
## 6. Conclusions and future perspectives

We showed that it is feasible to predict the properties of complex correlated materials such as cuprates with DFT, using the meta-GGA SCAN functional. This not only applies to compounds at ambient conditions but also under pressure or biaxial strain. The SCAN functional that was used in this work showed a very promising ability of reproducing phenomena that are far from trivial in these materials, encouraging further work to predict the physics of cuprates. The calculation of the critical temperature  $T_c$  and the strength of the pairing interaction that leads to superconductivity will be the future direction of the present thesis.

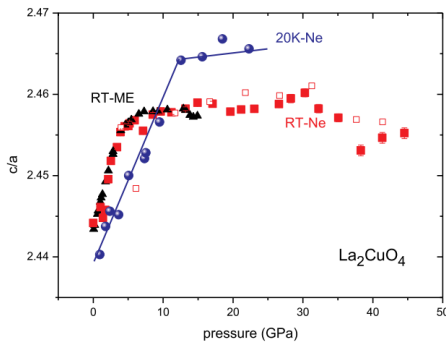
## 7. Acknowledgements

I would like to thank Prof. Gianni Profeta, who helped me throughout all of this thesis work and Prof. Giacomo Ghiringhelli and his group, who welcomed me in the physics department during these months of research.





(a) Theoretical prediction of the  $c/a$  normalized coefficient in LCO (defined as  $c/a = 2c/(a + b)$ ) with the SCAN functional. One can recognize the change of slope in the curve at 13 GPa.



(b) Measured  $c/a$  coefficient in LCO. Taken from Ref. [6]. The 20 K measurement is remarkably similar to the theoretical prediction.

Figure 8

## References

- [1] James W Furness, Yubo Zhang, Christopher Lane, Ioana Gianina Buda, Bernardo Barbiellini, Robert S Markiewicz, Arun Bansil, and Jianwei Sun. An accurate first-principles treatment of doping-dependent electronic structure of high-temperature cuprate superconductors. *Communications Physics*, 1(1):11, 2018.
- [2] Jianwei Sun, Adrienn Ruzsinszky, and John P Perdew. Strongly constrained and appropriately normed semilocal density functional. *Physical review letters*, 115(3):036402, 2015.
- [3] J-P Locquet, J Perret, J Fompeyrine, E Mächler, Jin Won Seo, and G Van Tendeloo. Doubling the critical temperature of

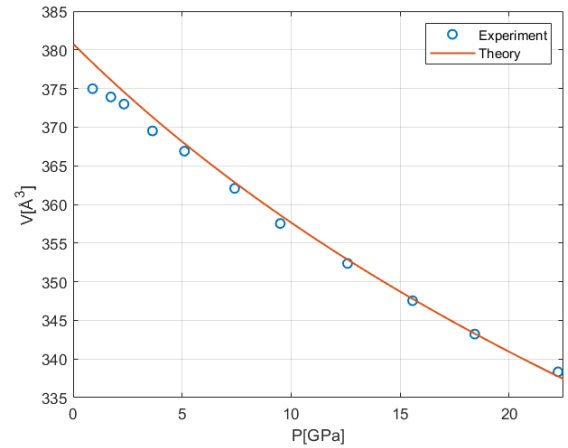


Figure 9: LTT equation of state. The points represent the experimental data, the continuous line the equation of state computed with the SCAN functional. The data are taken from Ref. [6].

la1. 9sr0. 1cuo4 using epitaxial strain. *Nature*, 394(6692):453–456, 1998.

- [4] O Ivashko, M Horio, W Wan, NB Christensen, DE McNally, E Paris, Y Tseng, NE Shaik, HM Rønnow, HI Wei, et al. Strain-engineering mott-insulating la2cuo4. *Nature communications*, 10(1):786, 2019.
- [5] SM Hayden, G Aeppli, R Osborn, AD Taylor, TG Perring, SW Cheong, and Z Fisk. High-energy spin waves in la 2 cuo 4. *Physical review letters*, 67(25):3622, 1991.
- [6] M Calamiotou, P Parisiades, E Siranidi, D Lampakis, K Conder, and E Liarokapis. Pressure induced lattice effects in pure and near optimally doped la2- xsrxcuo4. *Physica C: Superconductivity and its applications*, 565:1353516, 2019.